

Influence of parameters U and J in the LSDA+ U method on electronic structure of the perovskites LaMO_3 ($M = \text{Cr, Mn, Fe, Co, Ni}$)

Zhongqin Yang, Zhong Huang, Ling Ye, and Xide Xie

Surface Physics Laboratory (National Key Laboratory), Fudan University, Shanghai, 200433, China

(Received 11 May 1999)

The electronic structures of the perovskite oxides LaMO_3 ($M = \text{Cr, Mn, Fe, Co, and Ni}$) have been studied in the local-spin density approximation LSDA+ U method with the on-site Coulomb interaction parameter U varying from 0.0 to 10.5 eV, and exchange parameter J , from 0.35 to 0.95 eV. It is found that the splitting of the occupied spin-up bands and the corresponding unoccupied spin-down bands increases almost linearly with the increase of U , while the positions of the completely empty orbitals (both spin-up and -down bands are unoccupied) are not sensitive to the value of U . These features cause the gaps of the compounds to increase first with U , and then they can increase (LaFeO_3), decrease (LaCrO_3 and LaMnO_3) or even drop to zero (LaCoO_3). The local magnetic moments increase linearly with increasing U . After considering the on-site Coulomb interaction, the binding energies for the perovskites are lowered, and decrease with the increase of U . The exchange parameter J also influences the electronic properties, though not as strongly as that of the U . A group of values of U and J parameters, which can give results closer to that given by experiments, have been found. [S0163-1829(99)00144-7]

I. INTRODUCTION

In recent years, the *ab initio* band-structure methods based on the local-spin-density approximation (LSDA) were widely used to calculate the electronic structures of transition-metal perovskites $\text{La}_{1-x}D_x\text{MO}_3$ (the dopant D being a divalent alkaline earth metal Ca, Sr, Ba, and M being the 3d transition metal),¹⁻³ since those doped perovskites, such as $(\text{LaCa})\text{MnO}_3$, $\text{La}_{0.7}\text{Sr}_{0.3}\text{MnO}_3$, were found to have some rather rare properties such as the colossal magnetoresistance observed near the room temperature⁴ and temperature-dependent structural phase transitions induced by an external magnetic field.⁵ It has been shown, however, that the standard LSDA technique fails to reproduce the insulating behavior, or underestimate the energy gap, and give magnetic moments,^{2,3} which are too small for many perovskites. Since the 3d electron correlations, which are not considered properly in LSDA, are very important in transition-metal oxides,^{2,6} they should be taken into account more rigorously beyond the LSDA. Very recently, the LSDA+ U method^{7,8} was developed in which the on-site Coulomb interaction U of the localized d (or f) electrons, introduced from the Hubbard model, had been included very well. It has been proved that all the discrepancies with experiments of the LSDA mentioned above could be resolved or improved significantly by this approach.^{6,9}

It is known that the on-site Coulomb interaction of d - d electrons is screened by other non-3d electrons and affected by the hybridization between $M(3d)$ - $\text{O}(2p)$ and $M(4s)$ - $\text{O}(2p)$ electrons in LaMO_3 and the lattice relaxation effects in crystal.¹⁰ All those factors may reduce the value of the interaction constants U and J , where the exchange parameter J is also used in LSDA+ U and identified with the Stoner parameter I , which is about $U/10$ in magnitude.⁷ For example, the U_{at} for the bare Mn atom, of about 20 eV, is reduced to only about $U_{at}^{relax} \approx 12.8$ eV, when the relaxation

effects of the atomic shells are included. The value of U in the solid is further reduced if the screening by other electrons are considered; Some values reported in the literature are $U \approx 6.9$ eV for MnO (Ref. 7) and $U \approx 7.8$ eV for Mn in ZnTe.¹¹ It is still difficult to find a correct way to obtain the values of U and J for compounds,¹² and the parameters used in various calculations may be different. For the transition-metal perovskites LaMO_3 , Solovyev *et al.*⁹ have calculated systematically the on-site Coulomb U and exchange J parameters by the standard LSDA-constraint technique.¹¹ It was found that as the atomic number of the transition-metal increases from 22 (Ti) to 29 (Cu), U gradually increases from about 8.0 to 10.0 eV, which means the electronic correlations are stronger. It was also shown in Ref. 9 that J parameter increased slowly (around 1.0 eV) with the increase of the atomic number of M . The parameters used by Mizokawa *et al.*,¹³ however, are much smaller than that used by Solovyev. There exists at least 3.0 eV deviation for U parameters used them. For example, the U value for LaMnO_3 used by Solovyev was about 9.1 eV, while that used by Mizokawa was only 5.5 eV. Satpathy *et al.*¹ also calculated the U, J parameters, which were 10.1 and 0.88 eV, respectively, for LaMnO_3 . Obviously, it can be seen that there exist great discrepancies among those values used by various authors. Therefore, which value of U, J are more reasonable and how the values affect the electronic structures of LaMO_3 are problems to be investigated in the present work.

The different electronic structures of transition-metal perovskites LaMO_3 have been studied carefully by using the LSDA+ U method with U varying from 0.0 to 10.5 eV, J , from 0.3 to 0.95 eV. It is found that the splittings of the occupied spin-up bands and the corresponding unoccupied spin-down bands increase almost linearly with the increase of U , while the positions of the unoccupied spin-up and corresponding spin-down bands change little with the various U . The energy gaps for the perovskites increase with small U

(from zero to 3.5 eV), and when U is larger, the gap can increase, decrease, or even drop down to zero for different compounds. The local magnetic moment increases and the binding energy decreases almost linearly with the increase of U . The J effect, though not as strong as that of U , is also studied. A group of values of U, J parameters, which give results compared well with the experiments, have been found for the perovskites.

II. CRYSTAL STRUCTURES AND METHOD

All experimentally observed crystalline structures and magnetic phases^{14–16} were used for our calculations performed for LaMO_3 ($M = \text{Cr, Mn, Fe, Co, and Ni}$). Orthorhombic and rhombohedral structures were used for LaM_1O_3 ($M_1 = \text{Cr, Mn, Fe}$) and LaM_2O_3 ($M_2 = \text{Co, Ni}$), respectively. As for magnetic phases, A-type antiferromagnetic (A-AFM) and G-AFM were studied for LaMnO_3 and LaCr(Fe)O_3 , respectively. Both LaCoO_3 and LaNiO_3 have paramagnetic (PM) ground states. Due to the distortion, the orthorhombic structure unit cell has four formula units, while the rhombohedral one has two.

The self-consistent band structure has been calculated by using the atomic-sphere approximation–linear muffin-tin orbitals (ASA–LMTO) method,¹⁷ in which the on-site Coulomb interaction U correlation has been taken into account. Since the ASA–LMTO method is only accurate for closely packed structures, the interstitial sites in the unit cells for the compounds have been properly filled with empty spheres. Based on the original LSDA+ U method first proposed by Anisimov *et al.* in Ref. 7, the orbital-dependent one-electron potential used in our calculation has been written in the form

$$V_{m_1 m_2}^\sigma = \sum_{m'_1 m'_2} U_{m_1 m_2 m'_1 m'_2} (n_{m'_1 m'_2}^{-\sigma} - \bar{n}_{m'_1 m'_2}) + \sum_{m'_1 m'_2} (U_{m_1 m_2 m'_1 m'_2} - J_{m_1 m_2 m'_1 m'_2}) (n_{m'_1 m'_2}^\sigma - \bar{n}_{m'_1 m'_2}), \quad (1)$$

where m (m_1, m_2) and σ designate the orbital and spin, respectively. The orbital-flip amplitudes in the partial occupancies of d orbitals $n_{m_1 m_2}^\sigma$ (Ref. 18) have been considered in Eq. (1). And $\bar{n}_{m_1 m_2}$ is the $m_1 m_2$ -dependent average density; only averaging over spin is assumed here: $\bar{n}_{m_1 m_2} = (n_{m_1 m_2}^\uparrow + n_{m_1 m_2}^\downarrow)/2$. The matrix elements $U_{m_1 m_2 m'_1 m'_2}$, $J_{m_1 m_2 m'_1 m'_2}$ can be expressed in terms of complex spherical harmonics and effective Slater integrals F^k .¹⁹ For d electrons, only F^0 , F^2 , and F^4 are needed, and these can be related to the averaging Coulomb U and exchange J parameters via $U = F^0$ and $J = (F^2 + F^4)/14$ ($F^4/F^2 \approx 0.625$ for $3d$ elements).^{20,21} Thus, if the averaging parameters U, J are known, the F^0 , F^2 , and F^4 can be obtained through the above relations, and so are the two matrices $U_{m_1 m_2 m'_1 m'_2}$ and $J_{m_1 m_2 m'_1 m'_2}$.

It is obvious that if $n_{m_1 m_2}^\uparrow = n_{m_1 m_2}^\downarrow$ (paramagnetic phase or low-spin state, such as Co^{3+} in LaCoO_3), the fluctuation of charge density $n_{m_1 m_2}^\sigma (n_{m_1 m_2}^{-\sigma}) - \bar{n}_{m_1 m_2}$ in Eq. (1) is equal to zero, therefore there is no Hubbard-like interaction consid-

ered. Another scheme to consider the Hubbard term has been chosen to improve the results of LaCoO_3 and LaNiO_3 , which have paramagnetic ground state. It is the so-called spherical LDA+ U method,²² in which the matrix of the one-electron potential is given by

$$V_{m_1 m_2}^\sigma = V_{\text{LDA}} + (U - J) (\frac{1}{2} \delta_{m_1 m_2} - n_{m_1 m_2}^\sigma). \quad (2)$$

And the corresponding total energy is expressed as

$$E = E_{\text{LDA}} + \frac{U - J}{2} \left(\sum_{m\sigma} n_{mm}^\sigma - \sum_{m_1 m_2 \sigma} n_{m_1 m_2}^\sigma n_{m_2 m_1}^\sigma \right). \quad (3)$$

In Eq. (3), the interaction between electrons with opposite spins $U n^\uparrow n^\downarrow$ is not included; it has been canceled by the same term appearing in the corresponding double-counting energy, which represents the interaction energy between localized electrons considered in the standard LSDA. Thus, only the Coulomb interaction between the localized electrons with the same spin is considered in this scheme.

III. RESULTS AND DISCUSSION

The electronic structures of LaMO_3 ($M = \text{Cr, Mn, Fe, Co, and Ni}$) are first studied by the standard LSDA method ($U, J = 0.0$ eV in the calculation) to compare with the LSDA+ U results. It is found that LSDA cannot explain very well the electronic properties of the compounds, except for LaNiO_3 , which has metallic bands in low-spin ground state; the results obtained are in agreement with experimental results. In Tables I and II, the energy gaps and the magnetic moments calculated are listed, together with the experimental results. Since LaCoO_3 also lies in low-spin state (in the self-consistent process, the ferromagnetic state ultimately becomes paramagnetic), both LaCoO_3 and LaNiO_3 are not included in Table II. It is obvious that the LSDA cannot give reasonable band gaps for LaFeO_3 and LaCoO_3 and gives too small a gap for LaMnO_3 . The local magnetic moments at transition-metal ions in all compounds are underestimated (see Tables I and II). Therefore, to study those transition-metal perovskite oxides, it is important to include the on-site Coulomb interaction term.

It is known that the on-site Coulomb interaction U in a strong-correlated system can shift the LDA occupied orbitals about $-U/2$ and unoccupied ones by $U/2$,²¹ which lead to opening up a gap $\sim U$ for a single- d band system.⁷ One may then conclude that the gap of a strong-correlated system is directly related to the value of U , and it will always increase if U increases. However, it was found by the present work that the gaps of perovskites LaMO_3 did not simply increase with U . Figures 1(a) and 1(b) show how gaps and local magnetic moments in LaMO_3 vary with the parameter U , where the exchange parameter J is fixed at 0.95 eV. The solid lines have been used in the figures (also in Figs. 5 and 6) to connect the separate dots, which represent the calculated results corresponding to the different values of U (or J) taken in the calculation. The results obtained by the standard LSDA are also shown in Fig. 1 by ‘‘diamond’’ symbols. Compared with the LSDA results, it was obvious that by including the Hubbard-like interaction term the results can be improved significantly. Even if the on-site Coulomb interaction param-

TABLE I. The calculated energy band gaps (in eV) for the perovskites LaMO_3 ($M = \text{Cr-Co}$) obtained by LSDA and LSDA+ U approach, compared with experimental and other theoretical results. The U and J parameters used in the table are listed in Table III.

	LaCrO ₃ (G-AFM)	LaMnO ₃ (A-AFM)	LaFeO ₃ (G-AFM)	LaCoO ₃ (PM)
The present work (LSDA)	1.1	0.1	0.0	0.0
The present work (LSDA+ U)	2.6	1.0	2.1	0.3
Solovyev [LSDA+ U_2 (Ref. 9)]	1.2	0.2	0.2	0.2
Mizokawa [Hartree Fock (Ref. 13)]	4.5	3	4	3.5
Exp. (Ref. 25)	3.4	1.1	2.1	0.3

eter U is equal to zero, the little exchange parameter J also increases the gaps and the moments. It is found that gaps of the perovskite oxides all increase first with small values of U , and then the gap may increase (for LaFeO₃), or decrease (LaCrO₃ and LaMnO₃), or even drop down to zero (LaCoO₃) when U increases to a certain value. The gaps do not increase monotonously with the increase of U , as one would generally expect. These very distinct properties of each compound are mainly related to the different electronic configurations of the transition-metal ions in those compounds. The reasons can be given in details after analyzing the densities of states (DOS) for the compounds.

Figures 2, 3, and 4 give the total DOS and partial DOS of transition-metal ions of LaCrO₃, LaMnO₃, and LaFeO₃, respectively, with different values of U . [In Figs. 2(b), 2(c), and 2(d), the partial DOS of O $2p$ have also been shown.] The partial DOS of transition-metal ions in all compounds are indicated by the shaded areas in the figures. It is found that the interaction parameters U, J did not change much of the positions O $2p$ and La $5d$ orbitals, which are located in the energy range of $-6 \rightarrow 0$ eV and $3 \rightarrow 8$ eV (see Figs. 2–4), respectively. Thus, for compounds without considering the Hubbard-like interaction term, we did not set the Fermi level (E_F) at the zero point in the figures [see Figs. 2(a), 3(a), and 4(a)] in order to make the O $2p$ and La $5d$ orbitals occupying at the same energy region with the cases in which

the on-site U are considered and the comparison of the figures more clearly shown. From Figs. 2–4, it can be seen that the valence bands are mainly contributed by O- $2p$ and $M-3d$, which are mixed strongly with each other. And the lowest-lying unoccupied bands are mainly by the d bands, which also hybridize strongly with the O $2p$. Since the distortions of the crystalline structure are small, t_{2g} and e_g can be approximately used to represent the d bands. By comparing the partial DOS in the shaded areas in Figs. 2(a)–2(d) (also see Figs. 3 and 4), it can be concluded that the splitting between the *occupied* spin up and the *unoccupied* spin down of $t_{2g}(e_g)$ level increases almost linearly with U and the magnitude of the splitting is in the order of the U value. The total DOS of LaMnO₃ agrees with that obtained by Satpathy *et al.*¹

For LaCrO₃, the occupied bands of Cr ions are $t_{2g}^3 \uparrow$ and both $e_g \uparrow \downarrow$ orbitals are empty. Comparing Figs. 2(a) and 2(b), it is found that when a U of 3.0 eV and J of 0.95 eV are added, the occupied $t_{2g}^3 \uparrow$ and unoccupied $t_{2g}^3 \downarrow$ orbitals shift down and upwards by about 2.5 eV, respectively. And they both shift continuously with the increases of U . Such features of the half-filled orbitals (with *occupied* spin-up bands and *unoccupied* spin-down bands) reflect the essential point of the idea of LSDA+ U .⁷ For the completely unoccupied e_g^2 orbitals, the spin-up and -down bands shift down and up-

TABLE II. The calculated magnetic moments at M sites (in μ_B) for the perovskites LaMO_3 ($M = \text{Cr, Mn, Fe}$) obtained by LSDA and LSDA+ U , compared with experimental and other theoretical results. The values of U and J used in the table are listed in Table III.

	LaCrO ₃ (G-AFM)	LaMnO ₃ (A-AFM)	LaFeO ₃ (G-AFM)
The present work (LSDA)	2.5	3.3	3.5
The present work (LSDA+ U)	2.9	3.8	4.1
Solovyev [LSDA+ U_2 (Ref. 9)]	3.0	3.7	3.7
Mizokawa [Hartree Fock (Ref. 13)]	3.0	3.9	4.6
Experimental's	2.8 ± 0.2 (Ref. 26)	3.7 ± 0.1 (Ref. 15)	4.6 ± 0.2 (Ref. 26)

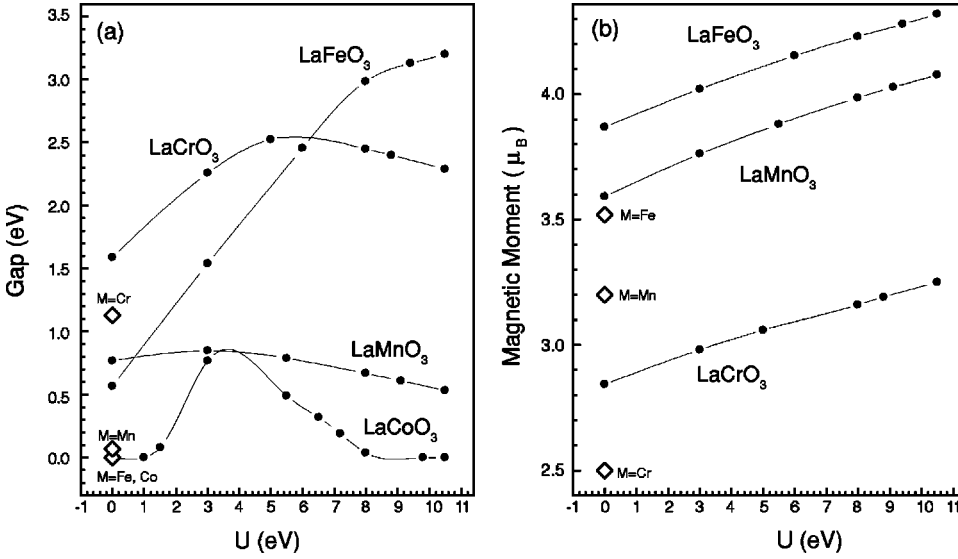


FIG. 1. (a) The variation of the gaps of perovskites LaMO_3 , $M = \text{Cr, Mn, Fe, and Co}$ with the on-site U parameter. (b) The variation of the magnetic moments at M ions in LaMO_3 , $M = \text{Cr, Mn, and Fe}$ with U . The exchange parameter J is fixed at 0.95 eV in the two figures. The “diamond” represent the results obtained by the standard LSDA.

wards, respectively, only by about 1.0 eV in Fig. 2(b), compared with the case of $U, J = 0.0$ eV in Fig. 2(a). And from Figs. 2(b)–2(d), it is found that the positions of e_g^2 hardly change with the increase of U . Since in the extremely localized limit $n_m \rightarrow 1$ or 0 (integral occupancy) the entirely empty orbitals are only affected by the exchange correlation interactions between the electrons with the same spin, the position of e_g^2 ($\uparrow\downarrow$) are only related to the exchange parameter J , not to U . And the shift of 1.0 eV of e_g^2 in Fig. 2(b) is of the order of $\frac{3}{2}J$ ($J = 0.95$ eV). It has been known from Fig. 1(a) that the gap of LaCrO_3 increases with U varying from 0.0 to 5.0 eV and then decreases slowly with the increase of U . From the partial DOS of O $2p$, which are indicated by the dotted lines, in Figs. 2(b), 2(c), and 2(d), it is found that the weight of the O $2p$ spectrum moves towards higher energy region (closer to E_F), and in Fig. 2(d), it is very clear that the O $2p$ bands have reached the top of valence. The high peaks of O $2p$ in Fig. 2(b) are mainly located from -5.0 to -1.0 eV and the top of valence band are mainly contributed by $t_{2g}^3\uparrow$, while in Fig. 2(c), O $2p$ bands together with $t_{2g}^2\uparrow$ contribute to the top of valence. Thus, it can be concluded that when the U added is small (< 5.0 eV), the top of the valence bands are mainly contributed by $t_{2g}^3\uparrow$, and the gap for LaCrO_3 is determined by the splitting between the $t_{2g}^3\uparrow$ and $e_g^2\uparrow$, where the $t_{2g}^3\uparrow$ always shifts sensitively to lower energy region with the increase of U (the corresponding compound is the so-called Mott-Hubbard-type insulator²³). Therefore, the gap for LaCrO_3 increases obviously with U increasing from 0.0 to 5.0 eV. When U continues increasing ($U \geq 5.0$ eV), due to O $2p$ bands becoming the top of the valence bands, the gap is mainly determined by the position of $e_g^2\uparrow$ band. (The gap belongs to charge-transfer type²³.) Due to the strong hybridization of Cr ($3d$)-O ($2p$) orbitals, some e_g electrons still occupy the Mn $3d$ orbital in the energy region hybridized with O $2p$'s. And it was found that the small occupancy of electrons at spin-up e_g^2 orbitals $n_{e_g^2\uparrow}^\uparrow$ increases with the increase of U , while $n_{e_g^2\uparrow}^\downarrow$ decrease ($n_{e_g^2\uparrow}^\uparrow > n_{e_g^2\uparrow}^\downarrow$, by about $0.3e$). From Eq. (1), it is known that the shift of potential of $e_g^2\uparrow$ orbital $\Delta V' = -U/2(n_{e_g^2\uparrow}^\uparrow - n_{e_g^2\uparrow}^\downarrow) - J/2[M - (n_{e_g^2\uparrow}^\uparrow - n_{e_g^2\uparrow}^\downarrow)]$, where M is the magnetic moment of

Cr^{3+} ions, which increases with U [see Fig. 1(b)]. Thus, with the increase of U (> 5.0 eV), the $e_g^2\uparrow$ orbital shifts slowly to lower energy region, which results in the decrease of the gap for LaCrO_3 , where U is larger than 5.0 eV as shown in Fig. 1(a). Due to the small deviation between the $n_{e_g^2\uparrow}^\uparrow - n_{e_g^2\uparrow}^\downarrow$, $\Delta V'$ decreases slowly with U , which lead to the gap for LaCrO_3 in Fig. 1(a) varying with a small slope.

The occupied bands of Mn ions in LaMnO_3 are $t_{2g}^3\uparrow e_g^1\uparrow$, and both the occupied $e_g^1\uparrow$ and $t_{2g}^2\uparrow$ orbital in Fig. 3 changes significantly with U . When a U of 3.0 eV and J of 0.95 eV is added, the $t_{2g}^2\uparrow$ orbital in Fig. 3(b) is located in the energy region below the O $2p$, while for LaCrO_3 in Fig. 2(b), the top valence bands are mainly contributed by $t_{2g}^3\uparrow$. This is due to the stronger correlation interaction in LaMnO_3 than in LaCrO_3 , which results in the gap for LaMnO_3 in Fig. 1(a) increasing at a smaller range of the value of U ($0 \sim 3.0$ eV) than in LaCrO_3 ($0 \sim 5.0$ eV). The unoccupied $e_g^1\uparrow$ band changes a little with increasing U in Figs. 3(b)–3(d), which is similar to that of LaCrO_3 . With the larger value of U , the gap of LaMnO_3 decreases slowly, which is just the same as that of LaCrO_3 .

Due to the half-filled of Fe ions ($t_{2g}^3\uparrow e_g^2\uparrow$) in LaFeO_3 , the spin-up bands are located below the E_F and the spin-down states are above the E_F in Fig. 4. From Fig. 1(a), it is seen that the characteristic of gap for LaFeO_3 changing with U is not similar to the case of LaCrO_3 and LaMnO_3 ; the gap in LaFeO_3 always increases with the increase of U , although the slope is not unique. The $3d$ orbitals of LaFeO_3 become very narrow and sharp (namely very localized) after adding a U of 3.0 eV and J of 0.95 eV in Fig. 4(b). From Figs. 2(b), 3(b), and 4(b), the positions of the occupied d states in the compounds move gradually to lower energy region [in Fig. 4(b), both the occupied $t_{2g}^3\uparrow e_g^2\uparrow$ are almost completely located below the O $2p$], which mean the correlation interaction between electrons increases in LaMO_3 with M varying from Cr to Fe. Since after considering the U interaction the top valence bands are mainly contributed by O $2p$, which is not sensitive to the U parameter, the gap of LaFeO_3 is determined by the position of the unoccupied $t_{2g}^3\downarrow$. In Fig. 4, the unoccupied $t_{2g}^3\downarrow$ orbitals move to higher energy region with

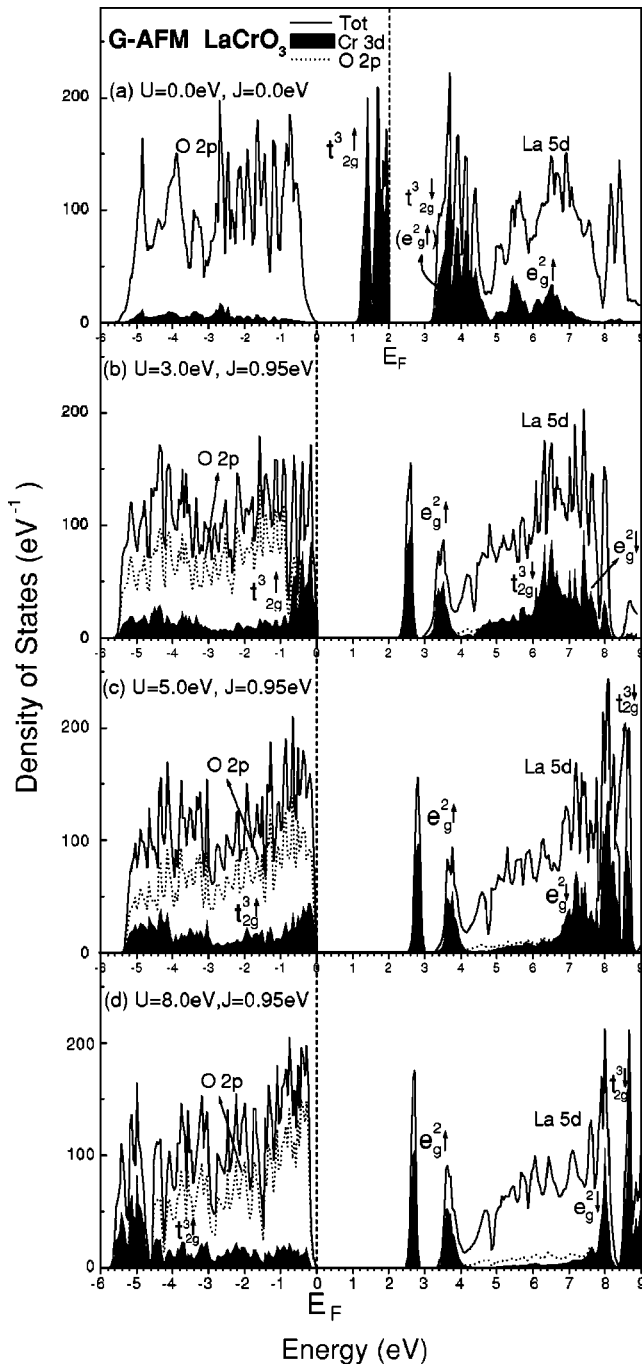


FIG. 2. The total and partial DOS of LaCrO₃ obtained by using different values of U : (a) without the on-site Coulomb interaction ($U, J=0.0$ eV); (b) $U=3.0$ eV; (c) $U=5.0$ eV; (d) $U=8.0$ eV. In (b), (c), and (d), J is fixed at 0.95 eV. The shaded areas indicate the partial DOS of Cr- d orbitals. The dotted lines in (b), (c), and (d) give the partial DOS of O $2p$ orbitals. And the vertical dash lines show the Fermi level.

U varying from 0.0 to 8.0 eV, which cause the gap increases almost linearly in Fig. 1(a) with U in the corresponding region. From the above discussion, it is found that although the gaps of LaFeO₃ and LaCrO₃ (LaMnO₃) all increase first with the increase of U , the mechanisms of causing the increase are different. The gap of LaFeO₃ increasing slowly when $U > 8.0$ eV may be due to the different on-site interaction strength between the t_{2g} and e_g electrons. It is known

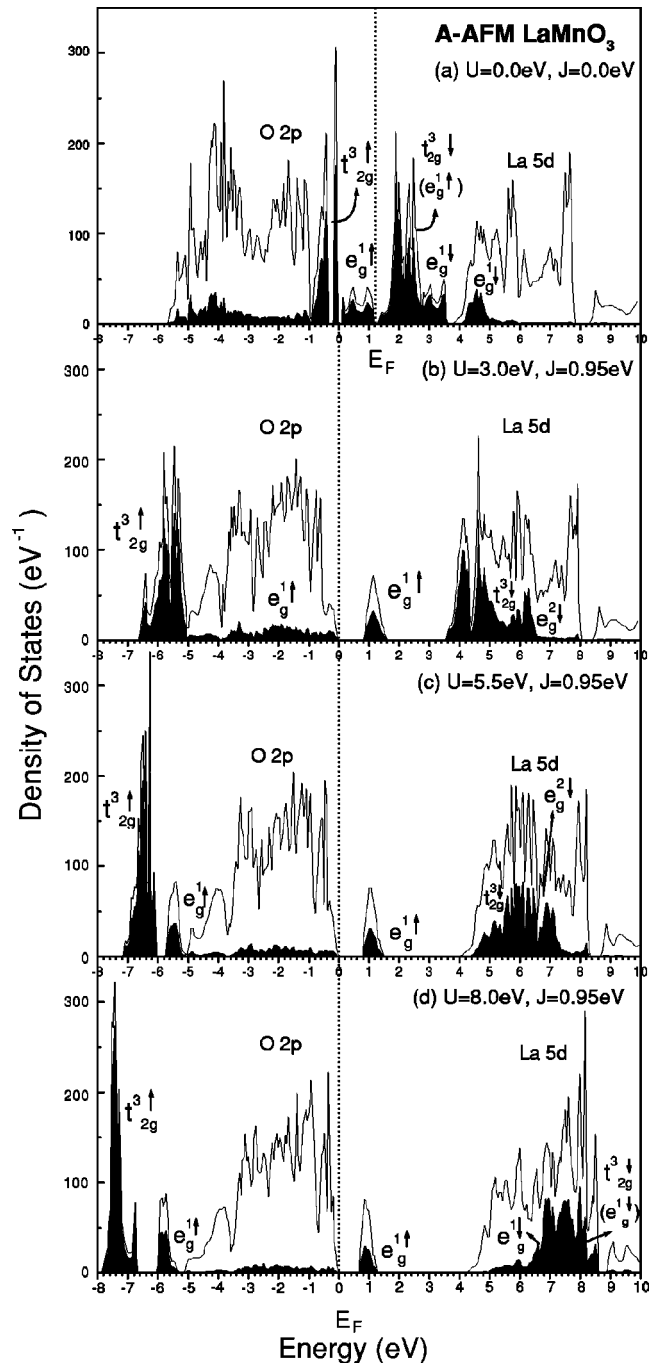


FIG. 3. The total and partial DOS of LaMnO₃ obtained by using different values of U : (a) without the on-site Coulomb interaction ($U, J=0.0$ eV); (b) $U=3.0$ eV; (c) $U=5.5$ eV; (d) $U=8.0$ eV. In (b), (c), and (d), J is fixed at 0.95 eV. The shaded areas indicate the partial DOS of Mn- d orbitals. The dotted line gives the Fermi level.

that the t_{2g} electrons have more localized property than e_g 's (Ref. 9) [$U(t_{2g}) > U(e_g)$], the t_{2g} orbitals are more sensitive to the values of the on-site U . In Fig. 4, the splitting between unoccupied e_g and t_{2g} becomes smaller with U increasing. That means the t_{2g} moves to high-energy region more quickly than e_g . Thus, when e_g becomes the lowest conduction bands, the gaps of LaFeO₃ will increase slowly.

Since all 3d electrons (t_{2g}, e_g) are supposed to be localized and influenced by the on-site Coulomb interaction, the position of the occupied d orbitals have large shift to lower

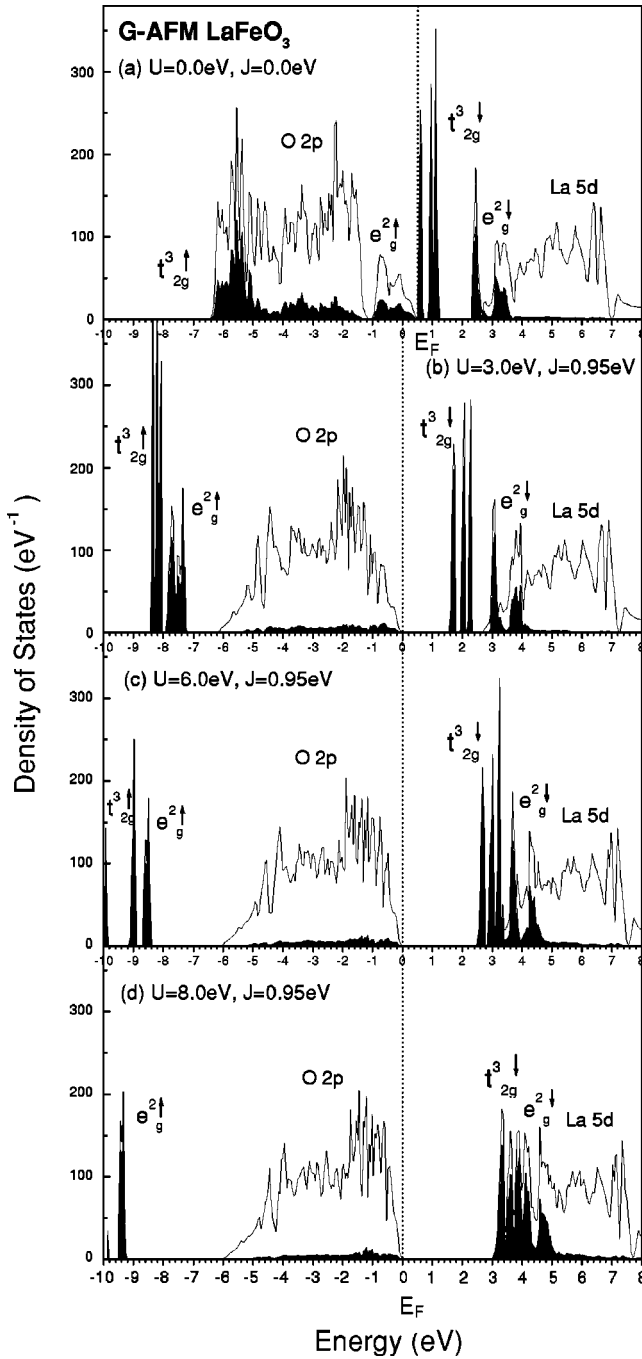


FIG. 4. The total and partial DOS of LaFeO_3 obtained by using different values of U : (a) without the on-site Coulomb interaction ($U, J=0.0$ eV); (b) $U=3.0$ eV; (c) $U=6.0$ eV; (d) $U=8.0$ eV. In (b), (c), and (d), J is fixed at 0.95 eV. The shaded areas indicate the partial DOS of Fe- d orbitals. The dotted line gives the Fermi level.

energy range, and even become lower than the O $2p$ when a larger U is considered. But, in experiment, it was found that the occupied e_g band is located above the O $2p$ for LaMnO_3 ,²⁴ which may be due to the itinerant property of e_g electron. Solovyev *et al.*⁹ have studied the perovskites by two LSDA+ U methods, in one method all d electrons were considered as localized ones, whereas in the other method only t_{2g} electrons were considered as localized, and the e_g ones were treated as itinerant in the scope of the standard LSDA approach. They believed that the second LSDA+ U_2

method provided more appropriate description for the perovskites. However, the LSDA+ U_2 did not give good results for gaps in the compounds (see Table I), although it described the position of e_g orbital well. In fact, it is impossible to separate precisely the electrons in the distorted crystal as t_{2g} and e_g because the distortion leads to the mixing between the two kind of electrons. Therefore, how to choose localized orbitals is a problem in the LSDA+ U program when dealing with transition-metal perovskite oxides.

Paramagnetic (PM) ground state has been studied for LaCoO_3 and LaNiO_3 . After taken the on-site Coulomb interaction into account, as shown in Eqs. (2) and (3), there are still bands across the E_F in LaNiO_3 , although the width of the valence band is larger and some of the d orbitals move away from E_F to lower energy region. LaNiO_3 having metallic bands is in agreement with experimental results. For LaCoO_3 , metallic bands were obtained by using the standard LSDA method [see Fig. 1(a)], while, in experiment, the insulating bands with a gap of 0.3 eV (Ref. 25) had been observed. When the on-site Coulomb interaction U was considered, the gap could be opened. In Fig. 1(a), the gap of LaCoO_3 (ionic configuration $t_{2g}^6 e_g^0$) appears when U reaches about 1.2 eV ($J=0.95$ eV). It increases to 0.85 eV when U is equal to 4.0 eV. Then the gap decreases, and drops to zero with the continuous increases of U . When the value of the on-site U parameter is about 6.5 eV, the PM LaCoO_3 has a gap of 0.3 eV. From Eq. (2), it is known that the gap should always increase with increasing U in the integral occupancy. In fact, there exists stronger hybridization between the transition-metal ions and oxygen, Co($3d$) and O($2p$) in LaCoO_3 than in compounds with transition-metal ions $M=\text{Cr, Mn, Fe}$, due to the short bond length of Co-O. Some electrons occupied the e_g bands, which should be empty in the case of integral occupancy. And more electrons would occupy the e_g bands with the increase of U . When the number of e_g electrons reaches a certain value, the potential of e_g orbital $V(e_g)$ in Eq. (2) becomes negative. The e_g orbital will then shift to the lower energy region; as a result, the gap will decrease and even drops to zero.

From Figs. 2–4, it can be seen that the exchange splitting between the occupied $t_{2g}\uparrow$ ($e_g\uparrow$) and unoccupied $t_{2g}\downarrow$ ($e_g\downarrow$) increases almost linearly with U . When the occupied $t_{2g}\uparrow$ ($e_g\uparrow$) levels moves to lower energy with the increase of U , they become more difficult to lose electrons. It has been found that there are more electrons occupying the $t_{2g}\uparrow$ ($e_g\uparrow$) bands. On the other hand, the little occupancy of spin-down electrons in the occupied states are found to be much smaller for LaMO_3 ($M=\text{Cr, Mn, Fe}$) with the increase of U . Those features cause the local magnetic moments of M in LaMO_3 perovskite increase linearly with U as shown in Fig. 1(b). The LSDA's results, shown by ‘‘diamond’’ symbols are also given in the figure for comparison. As shown in Table II, the magnetic moments of these compounds are significantly improved and are closer to the experimental results when the on-site Coulomb interaction U is considered. Since all the d orbitals are less than half-filled, the occupancy of electrons is the largest for Fe ion, and the least for Cr ion, the value of moment for Fe ion in the range of $3.8\text{--}4.5 \mu_B$ is also the largest, that of Cr ion being the least is about $3.0 \mu_B$, and that of Mn ion is in the middle and closer to that of Fe ion.

Figures 5(a) and 5(b) give the Hubbard energy, which

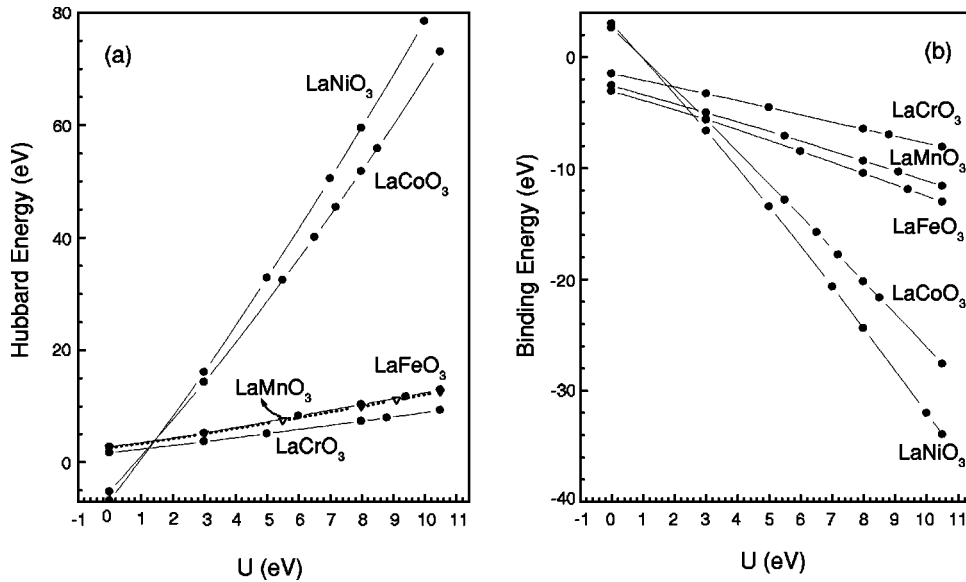


FIG. 5. (a) The Hubbard energies (per formula unit / M) for the perovskites versus the on-site parameter U . The small empty triangles on the dotted line give the results of LaMnO₃. (b) The binding energies (per formula unit / M) for the perovskites versus U , which are given by using the standard LSDA results as references.

reflects the strength of correlation interaction, and the binding energy (per formula unit / M) of LaMO₃ ($M = \text{Cr, Mn, Fe, Co, Ni}$), respectively. It is noted that there are similar features in the two figures. The small empty triangles on the dotted line in Fig. 5(a) represent the result of LaMnO₃. It is very close to that of LaFeO₃. The small disparity between the Hubbard energies of LaMnO₃ and LaFeO₃ may be due to the small difference between their structural constants.^{14,15} In Fig. 5(a), all the values of the Hubbard energy increase with U and the correlation interactions are stronger with the increase of the number of localized electrons (from Cr³⁺ to Ni³⁺), when U is not too small. In the case of LaCoO₃ and LaNiO₃, the energies are negative when U is in the range of about 0.0 to 1.0 eV and the energies of LaCoO₃ is higher than that in LaNiO₃, which are related to the property indicated in Eqs. (2) and (3). In general, the value of U is larger than that of J , and the correction term in Eq. (3), which can be written in a simpler form, $\Delta E = [(U - J)/2] \sum_{m\sigma} [n_{m\sigma}(1 - n_{m\sigma})]$, are positive. When $U < J$ ($J = 0.95$ eV), however, the correction term becomes negative, which cause the Hubbard energies of LaCoO₃ and LaNiO₃ becoming negative when U is in the range of 0.0 to 0.95 eV. The binding energies in Fig. 5(b) are given by using the results without the on-site Coulomb interaction as reference. It is found that the binding energies for the perovskites with the U, J interaction considered are lower than those obtained by the standard LSDA, and decrease with increasing U , except for the binding energies for LaCoO₃ and LaNiO₃ with U in the range of about 0.0 to 1.0 eV, which corresponds to the range in Fig. 5(a), where the Hubbard energies are negative for the two compounds. From Figs. 5(a) and 5(b), it can be seen that the higher the Hubbard energy is, the lower is the corresponding binding energy. It is known that the Hubbard interaction term added affects not only the total energy, but also the components of the total energy, such as the exchange correlation, traditional Coulomb, and kinetic energy. The structures should be more reasonably described by the LSDA+ U method. So, the binding energies may become lower when the on-site Coulomb U interaction is considered.

The affects of J on the gaps and the magnetic moments

are also studied in the present paper. We have fixed the U parameter equal to the values listed in Table III for the respective compounds, then varied the J parameters from 0.35 to 0.95 eV. The variations of gap and magnetic moment with J are shown in Figs. 6(a) and 6(b), respectively. The slopes of the curves in the two figures are smaller than those in Figs. 1(a) and 1(b) for U . Both the gaps and the magnetic moments shown in Fig. 6 vary almost linearly with the exchange parameters J . It is found that the splitting between the occupied spin-up and the unoccupied spin-down t_{2g} (e_g) levels increases with increasing J , similar to the effect of U mentioned above for LaMO₃ ($M = \text{Cr, Mn, Fe}$). Thus, in LaFeO₃ (the half-filled d orbital), the gap increases with the increase of J . It has been shown that gaps in LaCrO₃ and LaMnO₃ with larger value of U are determined by the positions of unoccupied $e_g \uparrow$ levels (see Figs. 2 and 3), which are related directly to the value of J . Since the unoccupied $e_g \uparrow$ band in LaCrO₃ shifts downwards by the order of $\frac{3}{2}J$, the gap of LaCrO₃ decreases with the increasing J in Fig. 6(a). The case for LaMnO₃ is similar to that of LaCrO₃. From Eqs. (2) and (3), where only the correction term with same spin is considered, it is known that the increase of J means the decrease of U when J is presumed to be unchanged. Consequently, the increase of the value of J from 0.35 to 0.95 eV for LaCoO₃ in Fig. 6(a) corresponds to the decrease of the value of U around 6.5 eV in Fig. 1(a), namely, the gap increases. Since the exchange splittings between the occupied $t_{2g}^3 \uparrow (e_g \uparrow)$ and the unoccupied $t_{2g}^3 \downarrow (e_g \downarrow)$ increase with both J and U , all the local magnetic moments of the transition-metal ions in LaMO₃ increase linearly with J , as shown in Fig. 6(b).

Since the on-site Coulomb interaction U and the exchange

TABLE III. A group of parameters U and J (in eV), which reproduce results close to that of experiments listed in Tables I and II.

	LaCrO ₃	LaMnO ₃	LaFeO ₃	LaCoO ₃	LaNiO ₃
U	5.0	5.5	6.0	6.5	7.0
J	0.5	0.5	0.6	0.65	0.65

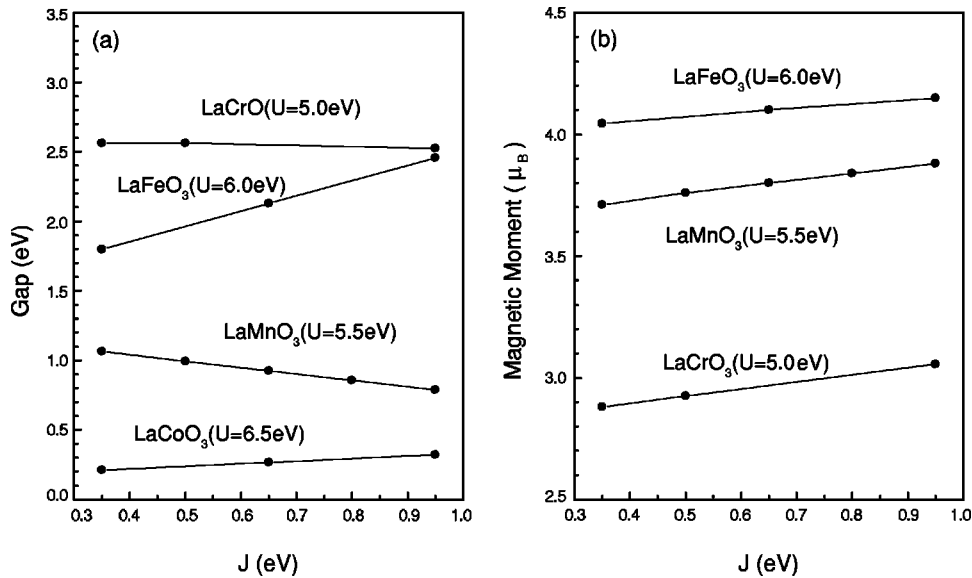


FIG. 6. (a) The gaps of perovskites LaMO_3 , $M = \text{Cr, Mn, Fe, and Co}$ versus the exchange parameter J . (b) The magnetic moments at M ions in LaMO_3 , $M = \text{Cr, Mn, and Fe}$ versus the J parameter. The parameter U in the different compound is fixed at a certain value as shown in the figures.

parameter J affect significantly on the electronic structures of the perovskites, it is very important to choose proper values of U and J in order to obtain results closer to the experimental results. Table III gives a group of parameters U and J for the perovskites, which give the LSDA+ U results listed in Tables I and II. By comparing with results obtained by the standard LSDA in Tables I and II, it is obvious that the LSDA+ U yields results on both gaps and magnetic moments which have better agreement with the experiment. The results are also compared with that of Mizokawa (by Hartree Fock method),¹³ and Solov'yev (by LSDA+ U).⁹ It is found that gaps given by Solov'yev⁹ are much less than the experimental values, on the other hand, Mizokawa's results¹³ are somewhat overestimated, while the present LSDA+ U results in Tables I and II agree much better with the experimental results. In Table III, the parameters U vary from 5.0 to 7.0 eV for perovskites from LaCrO_3 to LaNiO_3 , with J being of the order $U/10$. The magnitudes of the on-site U are smaller than those ever used by other researchers within the LSDA+ U framework (about 10.0 eV or larger).^{9,1} The values of U and J parameters may be reduced by various factors in the crystal (see Introduction) such as screening, hybridization, lattice relaxation and so on.

IV. CONCLUSION

The electronic structures of perovskites oxides LaMO_3 (with $M = \text{Cr, Mn, Fe, Co, and Ni}$) have been studied by two LSDA+ U methods with different U and J parameters. It is found that positions of O $2p$ and La $5d$ orbitals do not

change much when the on-site Coulomb interaction is considered. The splittings of the occupied spin up bands (such as $t_{2g}^3 \uparrow$) and the corresponding unoccupied spin down bands ($t_{2g}^2 \downarrow$) increase almost linearly with the increase of U , while positions of the entirely empty orbitals (such as $e_g^2 \uparrow \downarrow$ in LaCrO_3) are not sensitive to the value of U . These features cause the gaps of the compounds to not always increase with the increase of the on-site Coulomb U parameter; they can increase (LaFeO_3), decrease (LaCrO_3 and LaMnO_3) or even drop to zero (LaCoO_3) when U increases to a certain value. The local magnetic moments and the binding energies of the compounds are also affected significantly by the on-site U parameter. The magnetic moments increase linearly with U . After considering the U interaction, the binding energies are lower, and much lower with the increase of U . The influences of the exchange parameter J are weaker than that of U . A group of not very large values of U and J parameters, which can give energy gaps and magnetic moments closer to that given by experiments, have been presented in the present work.

ACKNOWLEDGMENTS

This work was supported by the National Natural Science Foundation of China (Grant No. 19677202), the National PAN-DENG project (Grant No. 95-YU-41), and the Foundation of National High Performance Computing Center, Shanghai, China. We also thank Dr. S. Y. Savrasov for making the LMTO+ U program available to us.

¹S. Satpathy, Z. S. Popović, and F. R. Vukajlović, Phys. Rev. Lett. **76**, 960 (1996).

²D. D. Sarma, N. Shanthi, S. R. Barman, N. Hamada, H. Sawada, and K. Terakura, Phys. Rev. Lett. **75**, 1126 (1995).

³W. E. Pickett and D. J. Singh, Phys. Rev. B **53**, 1146 (1996); G. Pari, S. M. Jaya, G. Subramoniam, and R. Asokamani, *ibid.* **51**,

16 575 (1995).

⁴S. Jin, T. H. Tiefel, M. McCormack, R. A. Fastnacht, R. Ramesh, and L. H. Chen, Science **264**, 413 (1994); R. Von Helmolt, J. Wecker, B. Holzapfel, L. Schultz, and K. Samwer, Phys. Rev. Lett. **71**, 2331 (1993).

⁵A. Asamitsu, Y. Moritomo, Y. Tomioka, T. Arima, and Y.

- Tokura, *Nature (London)* **373**, 407 (1995).
- ⁶M. A. Korotin, S. Yu. Ezhov, I. V. Solovyev, V. I. Anisimov, D. I. Khomskii, and G. A. Sawatzky, *Phys. Rev. B* **54**, 5309 (1996).
- ⁷V. I. Anisimov, J. Zaanen, and O. K. Andersen, *Phys. Rev. B* **44**, 943 (1991).
- ⁸M. T. Czyżyk and G. A. Sawatzky, *Phys. Rev. B* **49**, 14 211 (1994).
- ⁹I. Solovyev, N. Hamada, and K. Terakura, *Phys. Rev. B* **53**, 7158 (1996).
- ¹⁰B. Brandow, *Adv. Phys.* **26**, 651 (1977).
- ¹¹O. Gunnarsson, O. K. Andersen, O. Jepsen, and J. Zaanen, *Phys. Rev. B* **39**, 1708 (1989).
- ¹²W. E. Pickett, S. C. Erwin, and E. C. Ethridge, *Phys. Rev. B* **58**, 1201 (1998).
- ¹³T. Mizokawa and A. Fujimori, *Phys. Rev. B* **54**, 5368 (1996).
- ¹⁴S. Geller, in *Structure Reports*, edited by W. B. Pearson (N. V. A. Oosthoek's Uitgevers Mij, Utrecht, 1957), Vol. 21, p. 313.
- ¹⁵J. B. A. A. Elemans, B. Van Laar, K. R. Van der Veen, and B. O. Loopstra, *J. Solid State Chem.* **3**, 238 (1971).
- ¹⁶G. Thornton, B. C. ToField, and A. W. Hewat, *J. Solid State Chem.* **61**, 301 (1986).
- ¹⁷O. K. Andersen, *Phys. Rev. B* **12**, 3060 (1975); H. L. Skriver, *The LMTO Method* (Springer, Berlin, 1984); O. K. Andersen, Z. Pawłowska, and O. Jepsen, *Phys. Rev. B* **34**, 5253 (1986).
- ¹⁸A. I. Liechtenstein, V. I. Anisimov, and J. Zaanen, *Phys. Rev. B* **52**, R5467 (1995).
- ¹⁹B. R. Judd, *Operator Techniques in Atomic Spectroscopy* (McGraw-Hill, New York, 1963).
- ²⁰F. M. F. de Groot, J. C. Fuggle, B. T. Thole, and G. A. Sawatzky, *Phys. Rev. B* **42**, 5459 (1990).
- ²¹V. I. Anisimov, I. V. Solovyev, M. A. Korotin, M. T. Czyżyk, and G. A. Sawatzky, *Phys. Rev. B* **48**, 16 929 (1993).
- ²²S. L. Dudarev, G. A. Botton, S. Y. Savrasov, C. J. Humphreys, and A. P. Sutton, *Phys. Rev. B* **57**, 1505 (1998).
- ²³H. Takahashi, F. Munakata, and M. Yamanaka, *Phys. Rev. B* **53**, 3731 (1996).
- ²⁴J. H. Jung, K. H. Kim, K. J. Eom, T. W. Noh, E. J. Choi, J. Yu, Y. S. Kwon, and Y. Chung, *Phys. Rev. B* **55**, 15 489 (1997).
- ²⁵T. Arima, Y. Tokura, and J. B. Torrance, *Phys. Rev. B* **48**, 17 006 (1993).
- ²⁶W. C. Koehler and E. O. Wollan, *J. Phys. Chem. Solids* **2**, 100 (1957).